

MULTIPLE-MATERIAL POWDER BED FUSION MACHINE DEVELOPMENT: REDUCING CROSS-CONTAMINATION BETWEEN MATERIALS

Scott E. Snarr, Andres Najera, Joseph Beaman Jr., Derek Haas

Department of Mechanical Engineering, The University of Texas at Austin, Austin, TX 78712

Abstract

Powder bed fusion is an additive manufacturing technology capable of producing fully dense, high strength parts with complex geometries. However, it is currently only able to fabricate parts comprised of a single material. Multiple-material capabilities would allow for an added level of design complexity and the matching of material properties to the functional requirements of a part. In order to achieve this, a full redesign of the current powder deposition system is required. Previous attempts to implement multiple-material powder deposition systems encountered issues with controlling the dimensional accuracy in the build direction and cross-contamination between materials. This research integrates an angled blade leveling mechanism along with a nozzle-based powder deposition system to solve these problems. A design of experiments was run to identify significant leveling parameters and to quantify material cross-contamination. A deposition and leveling system that creates a uniform height multiple-material powder bed with no significant cross-contamination of materials is demonstrated.

Introduction

Additive manufacturing (AM) is a group of fabrication techniques characterized by the addition of material layer-by-layer to build up a part. These processes eliminate old manufacturing constraints allowing for new design freedoms, rapid prototyping, and the construction of highly complex geometries [1] [2] [3]. Currently, several AM methods possess the capability of producing multiple-material parts. This provides part designers an additional level of design complexity and the ability to match material properties to functional requirements in specific areas of a part [4] [5]. To date, many of the industry applications for multiple-material AM require complex metal parts with high strength and good material properties that the current multiple-material AM processes aren't able to manufacture. Multiple-material metal AM methods including material extrusion, material jetting, and binder jetting produce lower strength parts [2] [4] while sheet lamination operations are limited in the geometries that they can create [2]. Furthermore, directed energy deposition (DED) methods can produce high strength parts but have poor dimensional accuracy and a rough surface finish that requires post-build machining [2]. Powder bed fusion (PBF), by contrast, is capable of producing geometrically complex metal parts with high strengths, good dimensional accuracy, and significantly better surface finishes than DED methods [6] [7]. However, current powder bed fusion machines are limited to single material part production due to their powder deposition systems (PDS).

The powder bed fusion process starts with either a hopper dropping a layer of powder onto a plate or a powder feed piston rising to expose a single layer of powder. A counter-rotating roller or a recoater blade then spreads the produced layer of powder over top of an existing

powder bed. A laser then scans the cross section of the desired part onto the powder bed, melting the powder particles and fusing them together. The process is repeated layer-by-layer to build up a three dimensional part [2] [6]. Although capable of producing parts with a number of desirable features, parts manufactured by PBF are currently limited to a single material by the powder delivery systems. As mentioned previously, these delivery systems spread powder over the entire powder bed at once, offering no potential for multiple-materials. In response to this, researchers have already spent time developing alternative powder deposition methods for the PBF process that enable the production of multiple-material parts.

There is an abundance of powder dispensing methods that researchers considered when redesigning the PBF deposition system for depositing multiple materials. Yang et al. provided an extensive summary of these approaches with the pros and cons of each [8]. Lappo et al. tested the first multiple-material deposition system. This system used a roller to deposit a full layer of material A and then selectively melted regions of the powder bed. A vacuum was then used to remove the loose powder and a second roller then spread material B over the powder bed. Material B was then scanned and the process was repeated to build up a part [9]. Many years later Anstaett et al. used a similar approach [10]. However, this deposition technique resulted in high levels of cross-contamination between the materials as well as cracking in some parts caused by the foreign material particles [9] [10]. Several other studies developed multiple-material deposition systems but they were not capable of depositing two materials within a single layer, only alternating the material layer-by-layer [11] [12] or creating a continuous gradient in the build height direction [13] [14]. Researchers are still utilizing some of these techniques today, however, many have now adopted powder deposition by means of a vibrating capillary tube or nozzle.

Vibration induced powder deposition by nozzle allows for true multiple-material capabilities, the ability to vary material both within a layer and from layer to layer. Chianrabutra et al. provide a succinct summary of the development of this technology over the years [15]. In most systems intended for additive manufacturing, a set of nozzles or tubes are attached to a gantry system that can translate them in the X, Y, and Z directions. The nozzle output orifice is properly sized in relation to the powder's average particle diameter (R/r ratio) in order to create a powder-dispensing valve [16]. By correctly sizing this ratio, adhesive forces between particles and between the particles and the wall result in the formation of domes and arrested powder flow. Dome development is attributed to van der Waals forces, liquid bridges, and electrostatic interactions [16]. Vibration can then be used as an on/off control valve where powder flow only occurs when the vibration is on, continuously preventing the formation of the dome structures. There are many different variations to this style of powder deposition [17] but all of them function in this same general manner and are well studied. Additional work has been completed to provide mathematical equations estimating the deposited powder track height and width [18] as well as how varying parameters such as nozzle height from surface, nozzle velocity, and vibration amplitude affect the amount of powder deposited onto the powder bed [15] [19].

Although nozzle-based powder deposition has many advantages, there are a few issues that have been previously identified. One of the main concerns with powder deposition via nozzle is that the powder is deposited in individual tracks that when put next to each other form a series of ridges with high and lows. These ridges led to geometrical inaccuracies in the build

height direction [20] [21]. Additionally, when attempting to stop the powder flow by switching off the vibration, powder flow does not arrest immediately, leaving an overdose of powder at the end of the track. In order to eliminate these deficiencies and create a uniform height powder bed for scanning of the powder, a leveling device is needed. However, as mentioned earlier, previously tested multiple-material leveling methods resulted in significant cross-contamination of materials in the powder bed. To solve these issues, this research proposes an angled blade leveling mechanism designed to level a multiple-material powder bed without causing significant cross-contamination between the materials. A design of experiments is run to evaluate important parameters affecting the leveling mechanism's performance. Full deposition and leveling of a uniform height multiple-material powder bed with no significant cross-contamination of materials is demonstrated.

Machine Design

A custom built micro powder bed fusion machine was used for the entirety of the experiments performed during this research. The machine, presented below in Figure 1, was originally designed for the fabrication of Silicon Carbide but has since been adapted for powder bed fusion with metal powders (also known as selective laser melting). It is equipped with a 1064 nm wavelength, 20 W Ytterbium pulsed fiber laser from IPG Photonics. The collimated beam output from the laser is fed through a beam expander and into a Cambridge Technology ProSeries galvo scanner. An F-theta lens from Sill Optics with a focal length of 80 mm focuses the beam onto a 50 mm diameter piston. The laser, optics, and scanner are mounted on a laser arm that a lead screw translates in the vertical direction. This allows for adjustment of the laser spot size focused on the piston. That piston is driven by a PZS-90 elevation stage from MicronixUSA with a travel range of 35 mm. A custom designed stainless steel vacuum chamber, which can also be purged with an inert gas, houses the piston and elevation stage. ScanMaster Designer software is used for the creation of laser scan files and laser parameter selection.

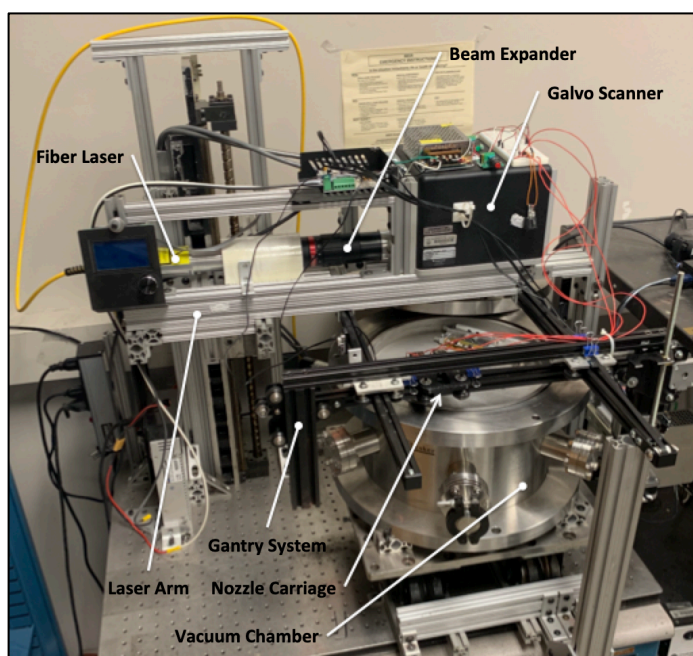


Figure 1. Micro powder bed fusion machine with integrated powder deposition system

The described micro PBF machine originally had a single material powder deposition system installed on it. In order to enable the selective deposition of multiple materials, a custom powder deposition system was designed and integrated. The powder deposition system (PDS), pictured in Figure 1 on the previous page, has two main parts, a gantry system and a carriage assembly. The gantry system is comprised mainly of a repurposed three-axis gantry system from a Creality Ender 3 (A low cost Fused Deposition Modeling 3D printer). Parts from the Creality Ender 3 were modified and reconfigured to fit onto the micro PBF machine in order to significantly decrease the design and manufacturing time of the PDS. The other half of the PDS, the carriage assembly, was additively manufactured and integrated with two powder deposition nozzles. It was designed to translate via the gantry system and selectively deposit the desired material at the correct instance. An eccentric rotating mass vibrational motor (#312-401 by Precision Microdrives), press fit into a housing on the front of each powder nozzle, is used to control the initiation and arrest of powder flow, similarly to the previously described nozzle-based powder deposition methods.

Once the powder deposition system was integrated with the micro PBF machine, deposition parameters were fine tuned for the precise deposition of Copper and Nickel powder. A 99.9% purity spherical Copper powder with a D50 of 10 – 15 μm produced by Stanford Advanced Materials was used along with a 99.8% purity spherical Nickel powder with a D50 of 10 – 15 μm produced by Edgetech Industries. These materials were chosen due to their compatibility and the desire to use them in subsequent research focusing on scanning strategy development for a Copper-Nickel multiple-material interface. Key parameters to tune include the translation speed of the nozzle, the vibrational amplitude used to maintain powder flow, and the distance of the nozzle output orifice from the deposition surface (nozzle standoff height). Additionally, the line spacing between consecutive tracks of powder is critical for creating a powder bed that is as close to a uniform thickness as possible. Table 1 below summarizes the final deposition parameters for both Copper and Nickel.

Table 1. Final deposition parameters for Copper and Nickel

	Nozzle Speed [mm/s]	Standoff Height [mm]	Vibrational Amplitude [g]	Line Spacing [mm]	Orifice Diameter [mm]
Copper	20.00	1.5	2.07	0.6	0.84
Nickel	52.67	1.5	2.13	0.9	1.04

Utilizing the determined deposition parameters, the multiple-material powder bed, seen on the next page in Figure 2, was deposited. The previously mentioned issues with nozzle-based powder deposition can be clearly seen in the Nickel region. The ridges formed from the powder tracks create an uneven powder surface while there are also additional mounds of powder at the end of each of the track caused by the acceleration and deceleration of the nozzle. These defects also occur in the Copper region but are not as clearly visible. In order to correct these issues and create a level, multiple-material powder bed for part fabrication, a novel leveling device was developed.

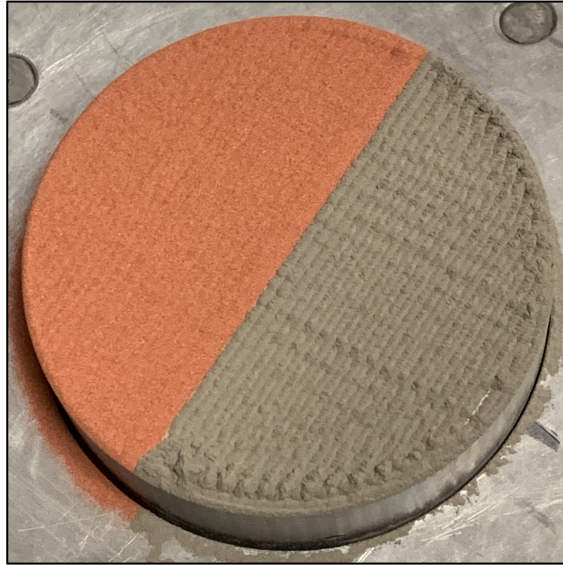


Figure 2. Deposited Copper-Nickel multiple-material powder bed

With knowledge gained from several initial prototypes, a final powder leveling device was integrated into the micro PBF machine. It can be seen below in Figure 3. The final leveling device consists of two main aluminum pieces and a steel shaft. All of these pieces were custom designed, hand machined, and then assembled using several commercial off the shelf parts. A long arm attaches the leveling device to the rotary hub of the micro PBF machine. It is secured to the hub by a screw. Additionally, the arm has mounting slots where two screws attach the other main aluminum piece, the blade holder. These slots allow for vertical adjustment of the blade holder to make sure the leading edge of the blade is always in contact with the leveling surface. The blade holder houses two tan bearings, press fit on each side to support a shaft and to allow rotary motion of the shaft. The leveling blade is attached to this shaft by two bolts. A thumb screw on the left side of the image provides fine adjustment of the blade angle while the vertical set screw on the left side locks and holds the blade angle after it has been set.

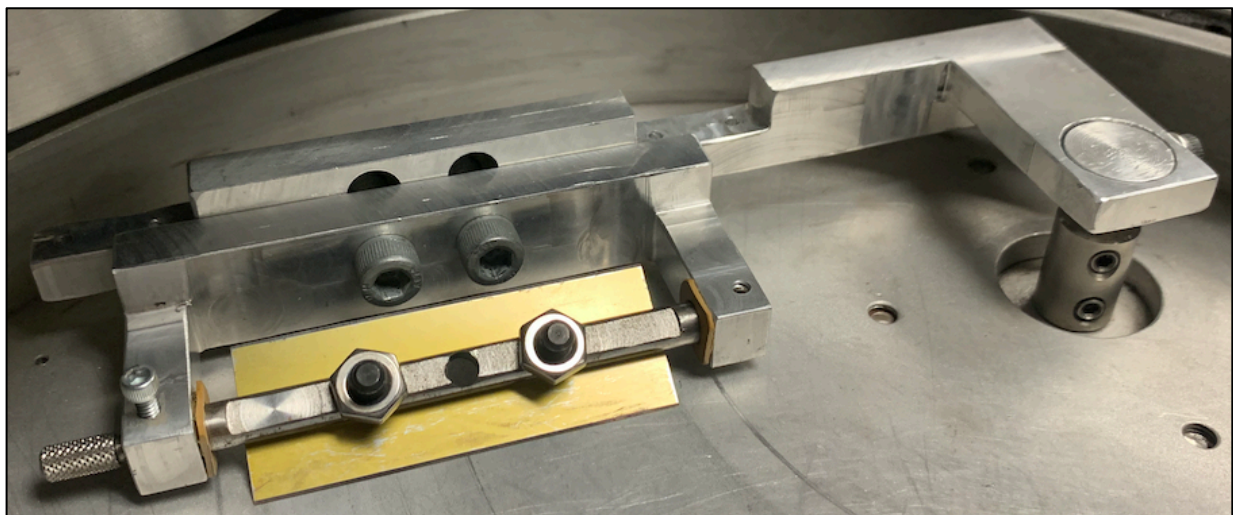


Figure 3. Final powder leveling device prototype

Experimental Methods

Initial testing showed the powder leveling device's effectiveness at removing excess powder to create a level powder bed. However, the other significant goal of the leveling device was to minimize the cross-contamination between materials during the leveling process. In order to quantify the material contamination and explore how several variables affect this contamination, a full design of experiments (DOE) was devised. There were two main variables that could be adjusted given the final leveling device's design and the micro PBF machine it was attached to. These two variables are the angle of the blade relative to the powder bed and the translation speed of the blade. Two main hypotheses were established for these design variables:

1. A smaller blade angle would increase the “cutting” action, therefore reducing material contamination
2. A faster translation speed would increase the “cutting” action, therefore reducing material contamination

Table 2 below shows the full design of experiments with each of the variables and the levels that were chosen for testing. Variable 1, blade angle, was defined as the angle of the centerline of the blade as measured from the horizontal powder bed. Six different levels were used for blade angle during the experiments; a 90° control group imitating current SLM recoater blades (blade perpendicular to powder bed) and five other levels ranging from 15° to 45° in increments of approximately 7.5°. Originally, blade angle was chosen to range from 15° to 45° in increments of 15°, however, after the initial experiments were performed, Trials 14 – 19 were added to fill in data gaps. Machine constraints limited the blade angle to angles above 15° but a manual leveling of a 0° blade angle, Trial 1, was performed. Trial 1 was excluded from most of the data analysis, as speed could not be precisely controlled with manual movement of the blade. However, interesting observations were made from this experiment that will be discussed later.

Table 2. Powder leveling device design of experiments

Trial #	Blade Angle [°]	Speed [mm/s]
1	0	X
2	15	21.5
3	15	59.5
4	15	83.3
5	30	21.5
6	30	59.5
7	30	83.3
8	45	21.5
9	45	59.5
10	45	83.3
11	90	21.5
12	90	59.5
13	90	83.3
14	22	21.5
15	22	59.5
16	22	83.3
17	37	21.5
18	37	59.5
19	37	83.3

MiniLog-Comm software by Phytron and a two phase stepper motor were used to control the second variable, the translation speed of the blade. This variable had three different levels that were tested, 21.5 mm/s (slow speed), 59.5 mm/s (medium speed), and 83.3 mm/s (fast speed). The slow speed was selected as the lowest speed the motor could move at while maintaining smooth movements. The fast speed was the highest speed of the motor that did not have acceleration or deceleration occurring while leveling the powder bed (wanted consistent speed during leveling).

The overall goal of this design of experiments was to quantify the effects that these two variables had on cross-contamination of materials during the leveling process. The output variable to be measured was, therefore, contamination percentage. To define contamination percentage, first look at Figure 4 below. After deposition, the Copper and Nickel regions each ideally cover half, or 50%, of the total area of the powder bed.

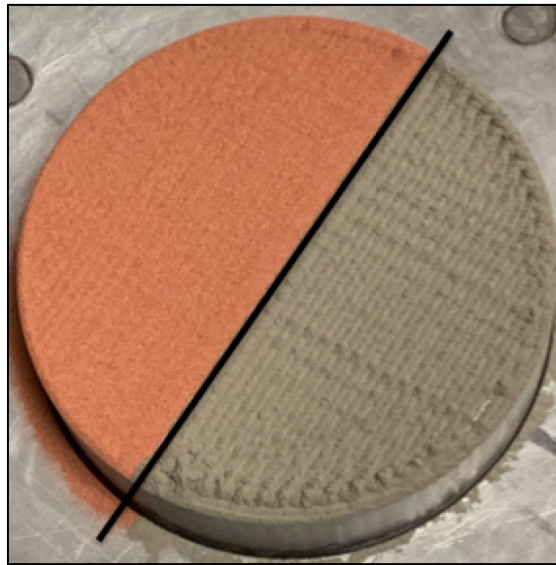


Figure 4. Ideal 50% Copper and 50% Nickel powder deposition

For these experiments, the blade first traveled over the Copper region and then over the Nickel region. The contamination percentage is defined as the percentage of the Nickel region that is occupied by Copper powder after leveling. No Copper powder in the Nickel region would equate to a 0% contamination percentage (50% Copper / 50% Nickel powder bed) while a 100% contamination percentage means the entire Nickel region is covered by Copper resulting in a 100% Copper powder bed. To summarize: contamination percentage only looks at the 50% deposited Nickel region of the powder bed and is the percentage of the Nickel area that Copper takes up after leveling.

To quantify the contamination percentage for each trial, a single image of the powder bed was captured after each run. This image was then processed using ImageJ, a public domain Java based image processing program. On the next page, Figure 5 depicts the entire data collection process for the contamination percentage of each trial. First, the image was uploaded to ImageJ and a yellow, circular region of interest (ROI) was drawn around the powder bed (Figure 5a).

The measure command was then used to calculate the area of that ROI (area of the entire powder bed). Next, the clear background command was used to remove excess powder around the powder bed that could skew the measurement (Figure 5b). After that, the color threshold tool was adjusted to select the entire Copper portion of the powder bed (Figure 5c). Finally, the color threshold was transferred to another yellow ROI that was then used to measure the total area of the Copper powder after leveling (Figure 5d). The area of Copper after leveling was used with the total initial area of the powder bed to calculate the contamination percentage for each of the leveling trials. It is important to note that several deposition trials were run to quantify the percentage of Copper and Nickel in the powder bed after deposition but before leveling (Instead of assuming 50/50). It was found that Copper occupied 51.39% of the powder bed initially, so a -1.39% correction factor was implemented to account for this.

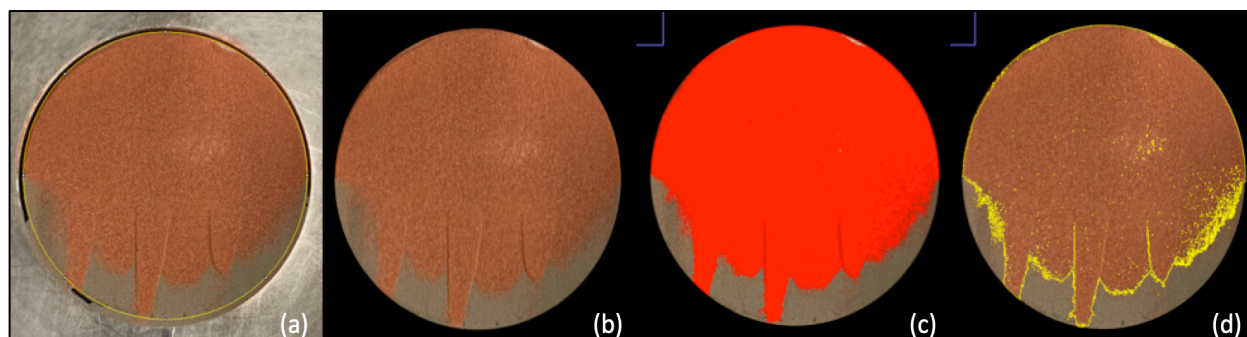


Figure 5. Sequential analysis performed in ImageJ to quantify contamination percentage, (a) Powder bed ROI selection, (b) Background removal, (c) Contamination selection with color threshold tool, (d) Selection of ROI for Copper contamination

Additionally, Figure 6 below shows the sensitivity of the ImageJ color threshold tool. It was able to accurately locate Copper contamination in the Nickel region that was difficult to see with the naked eye and otherwise would not have been detected. The yellow circle in Figure 6a shows a small amount of Copper contamination that was easily detected by the color threshold tool, shown in Figure 6b. The color threshold tool provided precise, automated detection of contamination in the deposited and leveled multiple-material powder bed.

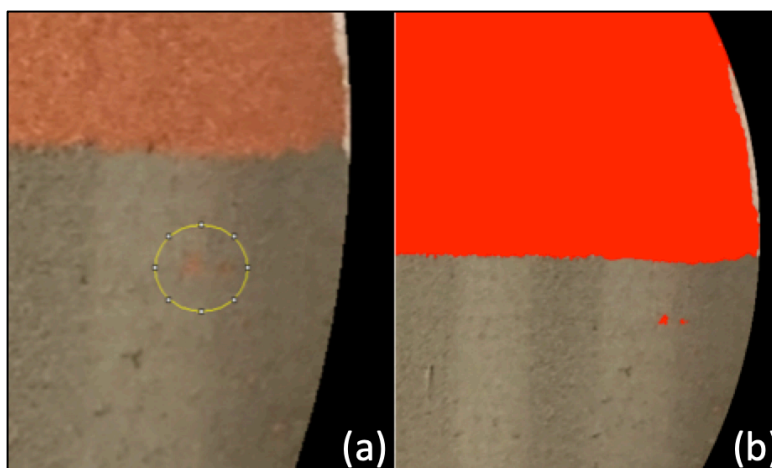


Figure 6. Demonstrated sensitivity of ImageJ color threshold tool, (a) Magnification of contamination, (b) Color threshold tool auto-detection of contamination

Experimental Results

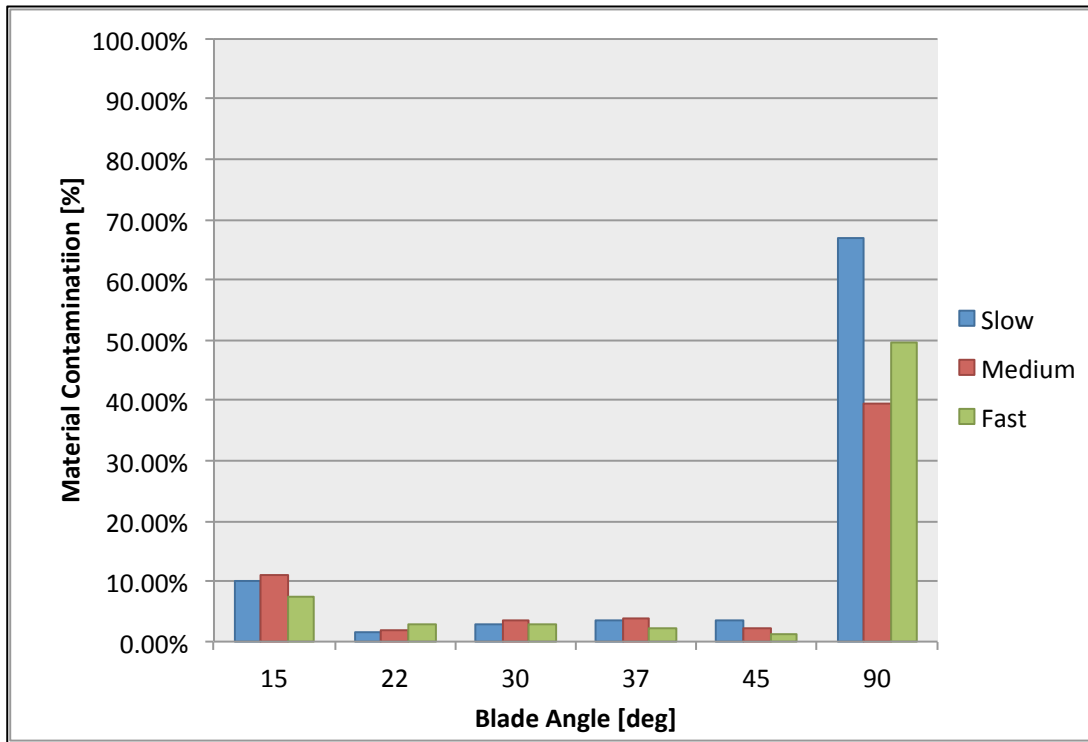


Figure 7. Final powder leveling device experimental results

Figure 7 above shows a summary of the completed experiments for testing the novel powder leveling device. The main goal of the leveling device was to reduce material contamination when compared to the traditional PBF machine's recoater blade or roller, defined as the 90° blade angle control group. A clear reduction in contamination is seen when comparing all of the angled blades to the 90° recoater blade. However, solely from the chart no conclusion on the most effective blade angle for reducing contamination can be drawn, as all blade angles between 22° and 45° are visually comparable. Additionally, when comparing the contamination difference due to blade speed, no clear trends can be seen in the chart. In order to quantitatively determine which of the variables were statistically significant, a two-factor ANOVA analysis was performed. The analysis was performed using Excel's Data Analysis ToolPak and a common alpha value of .05.

Table 3. Two-factor ANOVA analysis results

	F Value	F Critical	P Value	Alpha
Blade Angle	35.752	3.326	4.575E-06	0.050
Blade Speed	1.013	4.103	0.397	0.050

A two-factor ANOVA analysis tests the following two hypotheses:

1. H1: That the means of observations grouped by blade angle are the same
2. H2: That the means of observations grouped by blade speed are the same

On the previous page Table 3 presents the F statistics and P values associated with each of the variables. These metrics are used together to determine whether a variable's effect was statistically significant or occurred by chance. If the F value is less than the F critical value and the P value is higher than the alpha value of .05, the null hypothesis is accepted. This indicates the tested variable did not have a statistically significant effect on the measured contamination percentage. If the F value is greater than the F critical value and the P value is lower than the alpha value, the null hypothesis is rejected. This indicates the tested variable did have a statistically significant effect on the measured contamination percentage. Using this information, it can be seen from Table 3 that null hypothesis H1 is rejected and we accept null hypothesis H2. This means that blade angle had a statistically significant effect while blade speed did not. Interaction effects between the two variables were not explored as that would have required a significant increase in experimental time and was outside the scope of this research.

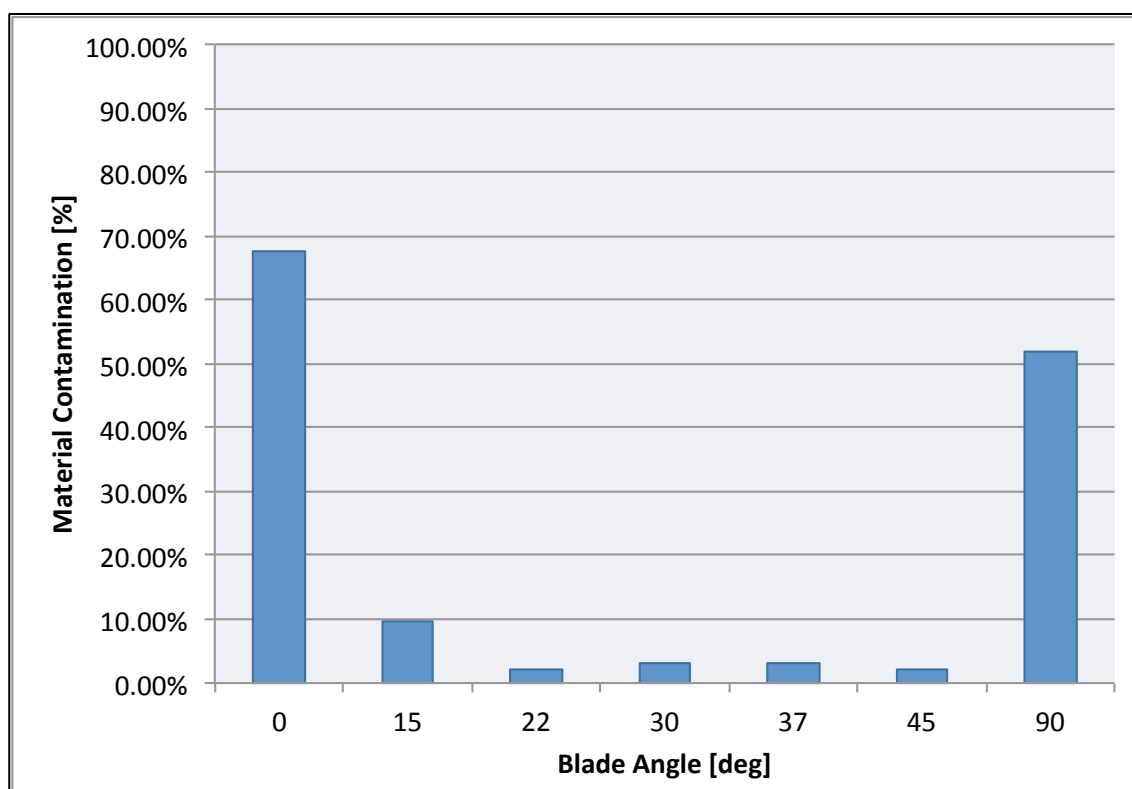


Figure 8. Quantification of material contamination for varying blade angles

Figure 8 shows the results from the final leveling experiments looking only at the effects of blade angle on the material contamination. The results of all the speed trials were averaged for display in this chart and the 0° blade angle trial was added. Both the 0° (blade parallel to the powder bed) and 90° blade angles resulted in significant contamination. The nominal thickness or height of the blade used was .02 mm, over 1000 times larger than the approximately 15 μ m particles it was spreading. Therefore, the 0° blade angle interacted with the powder the same as the 90° blade angle did, pushing the powder across the bed causing large amounts of cross-contamination. All of the angled blades showed significant reduction in material contamination when compared to the 0° and 90° trials. However, when a single factor ANOVA analysis was run for the other blade angles, it was found that there was no statistical difference in the material

contamination caused by blade angles of 22°, 30°, 37°, and 45°. Moving forward, the blade angle of 22° was used as it had the lowest average contamination percentage from the results of these experiments. Figure 9 below shows the final results of the development of the powder deposition system as well as the powder leveling device; a uniform height, contamination free multiple-material powder bed.

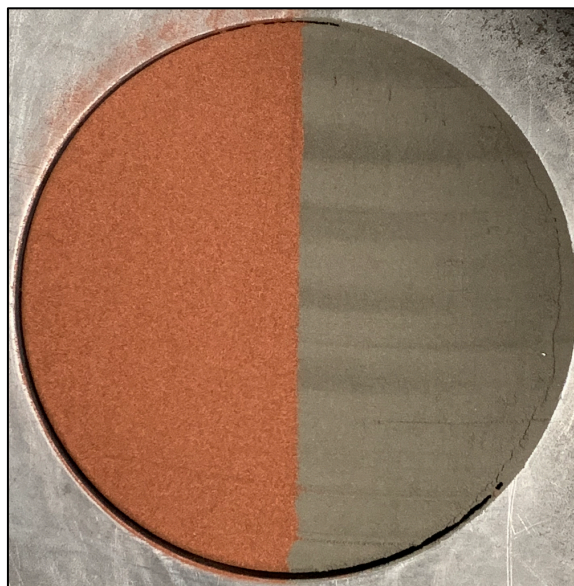


Figure 9. Level and contamination free multiple-material powder bed

One interesting effect that was discovered during the leveling experiments is the darker gray stripes in the Nickel region, seen above in Figure 9. The darker gray regions are where the Nickel powder has been very slightly raised. This is believed to be due to the fact that Nickel is ferromagnetic at room temperature. When the leveling blade is sliding across the surface, before it reaches the powder bed, friction forces create a build up of static charge on the blade. The moving static charge creates a magnetic field that the Nickel is then attracted to as it passes over. This causes the very top of the Nickel powder to slightly raise, resulting in the darker regions. It is not fully understood as to why the magnetism only affects some of the Nickel region and not the entire thing. This phenomena will be further explored in future research efforts.

Conclusion

The overarching goal of this research was to demonstrate the creation of a level, contamination free multiple-material powder bed. This was accomplished through the development of a nozzle-based powder deposition system that was integrated onto a custom micro PBF machine. The powder deposition system accurately delivered Copper and Nickel powder to the desired locations. A novel leveling device was then used to level the powder bed, removing excess powder to create a uniform height multiple-material powder bed free of cross-contamination between the materials. A full design of experiments was performed to test the effects of two parameters on the resulting material contamination. Translation speed of the blade was determined to not have a statistically significant effect on the material contamination in the powder bed while blade angle was determined to have a statistically significant effect. It was concluded that an angled leveling blade significantly reduced cross-contamination of the

materials when compared to traditional powder bed fusion roller and recoater blade mechanisms. A blade angle of 22° resulted in the lowest average material contamination of 2.04%. However, there was no statistically significant difference between the contamination results from blade angles 22°, 30°, 37°, and 45°. In summary, this research demonstrated creation of a level, contamination free multiple-material powder bed that will allow for future research to study scanning strategies for forming strong bonds in multiple-material part production.

Future Work

The research completed in this paper laid the foundation for many research projects in the future. The main goal of this research was to develop a powder deposition system capable of repeatedly creating a level, contamination free multiple-material powder bed. With this capability now in place, future studies can develop scanning strategies for creating strong bonds at multiple-material interfaces to enable multiple-material part production. Other future work includes the design and fabrication of a machine specifically built for multiple-material PBF, expanding studies on leveling parameters and their interaction effects, and also developing these leveling parameters for new material combinations.

Acknowledgement

This material is based upon work supported by the Department of Energy / National Nuclear Security Administration under Award Number(s) DE-NA0003921.

Disclaimer

This report was prepared as an account of work sponsored by an agency of the United States Government. Neither the United States Government nor any agency thereof, nor any of their employees, makes any warranty, express or implied, or assumes any legal liability or responsibility for the accuracy, completeness, or usefulness of any information, apparatus, product, or process disclosed, or represents that its use would not infringe privately owned rights. Reference herein to any specific commercial product, process, or service by trade name, trademark, manufacturer, or otherwise does not necessarily constitute or imply its endorsement, recommendation, or favoring by the United States Government or any agency thereof. The views and opinions of authors expressed herein do not necessarily state or reflect those of the United States Government or any agency thereof.

References

- [1] Gibson, I., Rosen, D. W., & Stucker, B. (2009). *Additive Manufacturing Technologies: Rapid Prototyping to Direct Digital Manufacturing*. Springer.
- [2] Ngo, T. D., Kashani, A., Imbalzano, G., Nguyen, K. T., & Hui, D. (2018). Additive manufacturing (3D printing): A review of materials, methods, applications and challenges. *Composite Part B: Engineering*, 143, 172-196.
- [3] Abdulhameed, O., Al-Ahmari, A., Ameen, W., & Mian, S. H. (2019). Additive manufacturing: Challenges, trends, and applications. *Advances in Mechanical Engineering*, 11, 1-27.
- [4] Vaezi, M., Chianrabutra, S., Mellor, B., & Yang, S. (2013). Multiple material additive manufacturing - Part 1: a review. *Virtual and Physical Prototyping*, 8, 19-50.
- [5] Loh, G. H., Pei, E., Harrison, D., & Monzon, M. D. (2018). An overview of functionally graded additive manufacturing. *Additive Manufacturing*, 23, 34-44.
- [6] Verma, R., & Kaushal, G. (2019). State of the Art of Powder Bed Fusion Additive Manufacturing: A Review. *3D printing and Additive Manufacturing Technologies*, 269-279.
- [7] Vartanian, K., Brewer, L., Manley, K., & Cobbs, T. (2018). *Powder Bed Fusion vs. Directed Energy Deposition Benchmark Study: Mid-Size Part with Simple Geometry*. Retrieved from https://optomec.com/wp-content/uploads/2018/06/PBF-vs-DED-BENCHMARK-STUDY_7March_2018-03.pdf
- [8] Yang, S., & Evans, J. (2007). Metering and dispensing of powder; the quest for new solid freeforming techniques. *Powder Technology*, 178, 56-72.
- [9] Lappo, K., Jackson, B., Wood, K., Bourell, D., & Beaman, J. (2003). Discrete Multiple Material Selective Laser Sintering (M2SLS): Experimental Study of Part Processing. *Solid Freeform Fabrication Symposium*, (pp. 109-119).
- [10] Anstaett, C., Dr.-Ing, Seidel, C., & Prof. Dr.-Ing G. Reinhart. (2017). Fabrication of 3D Multi-material Parts Using Laser-based Powder Bed Fusion. *Solid Freeform Fabrication Symposium*, (pp. 1548-1556).
- [11] Liu, Z. H., Zhang, D. Q., Sing, S. L., Chua, C. K., & Loh, L. E. (2014). Interfacial characterization of SLM parts in multi-material processing: Metallurgical diffusion between 316L stainless steel and C18500 copper alloy. *Materials Characterization*, 94, 116-125.
- [12] Sing, S. L., Lam, L. P., Zhang, D. Q., Liu, Z. H., & Chua, C. K. (2015). Interfacial characterization of SLM parts in multi-material processing: Intermetallic phase formation between AlSi10Mg and C18400 copper alloy. *Materials Characterization*, 107, 220-227.

- [13] Demir, A. G., & Previtali, B. (2017). Multi-material selective laser melting of Fe/Al-12Si components. *Manufacturing Letters*, 11, 8-11.
- [14] Nadimpalli, V. K., Dahmen, T., Valente, E. H., Mohanty, S., & Pedersen, D. B. (2019). Multi-material additive manufacturing of steels using laser powder bed fusion. In C. Nisbet, R. K. Leach, D. Billington, & D. Phillips (Eds.), *Proceedings of the 19th International Conference and Exhibition (EUSPEN 2019)* (pp. 240-243). The European Society for Precision Engineering and Nanotechnology.
- [15] Chianrabutra, S., Mellor, B., & Yang, S. (2014). A Dry Powder Material Delivery Device for Multiple Material Additive Manufacturing. *Solid Freeform Fabrication Symposium*, (pp. 36-48).
- [16] Yang, S., & Evans, J. R. (2004). Acoustic control of powder dispensing in open tubes. *Powder Technology*, 139, 55-60.
- [17] Lu, X., Yang, S., & Evans, J. R. (2009). Microfeeding with different ultrasonic nozzle designs. *Ultrasonics*, 49, 514-521.
- [18] Yang, S., & Evans, J. R. (2004). A Multi-Component Powder Dispensing System for Three Dimensional Functional Gradients. *Materials Science and Engineering A*, 379, 351-359.
- [19] Lu, X., Yang, S., Chen, L., & Evans, J. R. (2006). Dry Powder Microfeeding System for Solid Freeform Fabrication. *Solid Freeform Fabrication Symposium*, (pp. 636-643).
- [20] Wei, C., Li, L., Zhang, X., & Chueh, Y.-H. (2018). 3D printing of multiple metallic materials via modified selective laser melting. *CIRP Annals - Manufacturing Technology*, 67, 245-248.
- [21] Al-Jamal, O. M., Hinduja, S., & Li, L. (2008). Characteristics of the bond in Cu-H13 tool steel parts fabricated using SLM. *CIRP Annals*, 57, 239-242.